

Zeta-regularized vacuum expectation values from quantum computing simulations

Karl Jansen*

NIC, DESY Zeuthen, Platanenallee 6, 15738 Zeuthen, Germany

E-mail: karl.jansen@desy.de

Tobias Hartung

Department of Mathematics, King's College London, Strand, London WC2R 2LS, United Kingdom

E-mail: tobias.hartung@kcl.ac.uk

The zeta-regularization allows to establish a connection between Feynman's path integral and Fourier integral operator zeta-functions. This fact can be utilized to perform the regularization of the vacuum expectation values in quantum field theories. In this proceeding, we will describe the concept of the zeta-regularization, give a simple example and demonstrate that quantum computing can be employed to numerically evaluate zeta-regulated vacuum expectation values on a quantum computer.

*37th International Symposium on Lattice Field Theory - Lattice2019
16-22 June 2019
Wuhan, China*

*Speaker.

1. Introduction

One of the most fundamental concepts in theoretical physics is the path integral (or partition function in statistical physics) introduced by Feynman [1, 2] which can provide expectation values

$$\langle \Omega \rangle = \lim_{T \rightarrow \infty + i0^+} \frac{\text{tr}(U(0, T)\Omega)}{\text{tr}(U(0, T))} \quad (1.1)$$

of important observables Ω in high energy physics, statistical mechanics and beyond, e.g. in turbulence [3]. In eq. (1.1) $U(0, T)$ is the time evolution operator of a given physical system

$$U(0, T) = \text{Texp} \left(-\frac{i}{\hbar} \int_0^T H(\tau) d\tau \right), \quad (1.2)$$

with Texp denoting time ordered exponential and H the Hamiltonian of the considered physical model.

A major drawback of the path integral as written in eq. (1.1) is, however, that it is ill defined in general. A well known way out is to formulate the path integral on a discrete space-time lattice in Euclidean time, see e.g. the textbooks in [4, 5]. Although this approach of *lattice field theory* has been and is still extremely successful in computing physical quantities in QCD and other models of high energy physics, it is very limited in addressing e.g. real time phenomena, questions with a non-zero baryon density or CP violation related to matter anti-matter asymmetry of the universe. These are very important physical questions where, however, a sign problem appears such that standard Markov chain Monte Carlo methods are not suitable. It would therefore be very important and useful to find a regularization of the path integral in a Lorentzian background metric which holds non-perturbatively and which leads to a practical way to evaluate expectation values in the path integral formalism. If such a formalism could be extended to even more general metrics, e.g. curved space, then it would lead to an even more powerful exploitation of the path integral. In this proceeding, following refs. [6, 7, 8], we present a proposal to provide exactly such a setup. In particular, there are two main messages to convey:

- By a suitable ζ -regularization of the path integral we will obtain a mathematically sound, non-perturbative definition of the path integral which holds in very general metrics and, vacuum expectation values computed within this framework are *physical expectation values*.
- For the evaluation of the so defined expectation values quantum computations can be used on newly emergent quantum devices.

2. ζ -regularization

In order to pave the way towards the path integral in the ζ -regularization, we remind the reader of the Riemann ζ -function $\zeta_{\text{R}}(z)$ which is given by

$$\zeta_{\text{R}}(z) = \sum_{n=1}^{\infty} \frac{1}{n^z}, \{z \in \mathbb{C}; \Re(z) > 1\}. \quad (2.1)$$

If we analytically continue $\zeta_{\text{R}}(z)$, e.g. through the Γ -function, we receive a mathematically well defined definition of $\zeta_{\text{R}}(z)$ for $z \neq 1$. In particular, we can choose $z = -1$ to find

$$\zeta_{\mathbb{R}}(-1) = -\frac{1}{12}. \quad (2.2)$$

Although this is clearly a mathematically sound and well controlled result, it is rather counter intuitive. At $z = -1$ the series in eq. (2.1) is obviously divergent, but nevertheless we obtain a finite number at $z = -1$. This is surprising and we will come back to this ‘‘mystery’’ when we discuss the physical meaning of expectation values of observables in the ζ -regularized path integral.

The concept of the Riemann ζ -function can be extended to operators. Let us look for example at a simple infinite dimensional derivative operator on the torus $\mathbb{R}/2\pi\mathbb{Z}$,

$$\text{tr}|\partial| \stackrel{\text{F.T.}}{=} \sum_{n=-\infty}^{+\infty} |n| = 2 \sum_{n=1}^{\infty} n \quad (2.3)$$

where we performed a Fourier transformation (F.T.) to obtain the sum on the right hand side representing the trace of the operator. Again, being divergent, the series in eq. (2.3) is ill defined.

It is, however, possible to define a ζ -trace by introducing a holomorphic family of operators $\varphi(z)$

$$\varphi(z) := |\partial|^{1+z} \quad (2.4)$$

which for $\text{Re}(z) < -2$ has as a trace

$$\text{tr}\varphi(z) = 2 \sum_{n=1}^{\infty} n^{1+z}. \quad (2.5)$$

As in the example of the Riemann ζ -function, the series in eq. (2.5), which represents the trace of the operator $\varphi(z)$, can be extended analytically to define the operator ζ -function $\zeta(\varphi)(z)$ and $\text{tr}|\partial|$ can be evaluated using the induced ζ -trace

$$\zeta(\varphi)(z) = 2\zeta_{\mathbb{R}}(-z-1) \Rightarrow \text{tr}|\partial| := \zeta(\varphi)(0) = 2\zeta_{\mathbb{R}}(-1) = -\frac{1}{6}. \quad (2.6)$$

Again, we obtain a well defined value for the ζ -trace of the derivative operator but it is certainly not clear at all what the physical interpretation of this result would be.

Let us, in the next step, apply the above ideas to the quantity we are interested in, i.e. the time evolution operator

$$U(0, T) = \text{Texp} \left(-\frac{i}{\hbar} \int_0^T H(\tau) d\tau \right). \quad (2.7)$$

This time evolution operator has a Fourier integral kernel

$$k(x, y) = \int dr \int d\omega(\xi) e^{ih_2(x, y, \xi)r^2 + ih_1(x, y, \xi)r} a(x, y, r, \xi) \quad (2.8)$$

where we integrate over the spherical coordinates ($d\omega(\xi)$) and the radial components (dr) separately. In eq. (2.8) h_1 (h_2) correspond to first (second) order differential operators in the Hamiltonian and the $a(x, y, r, \xi)$ represent the ‘‘Fourier coefficients’’.

Using the time evolution operator of eq. (2.8) we can *formally* define the trace

$$\mathrm{tr}(U(0, T)) = \int dx \int dr \int d\omega(\xi) e^{ih_2(x, x, \xi)r^2 + ih_1(x, x, \xi)r} a(x, x, r, \xi) \quad (2.9)$$

which in general is ill defined since the trace can be (and usually is) divergent. However, following the spirit of the previous examples, we can introduce a family of holomorphic functions $g(z)$ obeying $g(0) = 1$ which will eventually be used to define the ζ -trace of the Fourier integral kernel. Examples of such functions are the choices $g(z) \propto r^z$. But, in principle, $g(z)$ can have a much more general form, see e.g. section (2.2). In mathematical language, introducing $g(z)$ means to “gauge” the integral kernel

$$k_g(x, y)(z) = \int dr \int d\omega(\xi) e^{ih_2(x, y, \xi)r^2 + ih_1(x, y, \xi)r} (ag(z)(x, y, r, \xi)) \quad (2.10)$$

which allows to define the ζ -trace of the Fourier integral kernel and hence, in turn, the time evolution operator

$$\begin{aligned} \mathrm{tr}_\zeta(U(0, T)) &= \zeta(k_g(x, y))(z)|_{z=0} \\ &= \int dx \int dr \int d\omega(\xi) e^{ih_2(x, x, \xi)r^2 + ih_1(x, x, \xi)r} (ag(z)(x, x, r, \xi))|_{z=0}. \end{aligned} \quad (2.11)$$

In a more general setup, as shown in ref. [6], a family of operators $\mathfrak{G}(z)$ with the property $\mathfrak{G}(0) = 1$ is introduced, *gauging* the time evolution operator to be of the form $U(T, 0)\mathfrak{G}(z)$. This too leads to the gauged Fourier integral kernel of eq. (2.10) with the corresponding ζ -trace of eq. (2.11), which in turn allows us to define a ζ -regulated vacuum expectation value

$$\langle \Omega \rangle := \langle \Omega \rangle_\zeta := \langle \Omega \rangle_{\mathfrak{G}(0)} := \lim_{z \rightarrow 0} \lim_{T \rightarrow \infty + i0^+} \frac{\mathrm{tr}(U(0, T)\mathfrak{G}(z)\Omega)}{\mathrm{tr}(U(0, T)\mathfrak{G}(z))}. \quad (2.12)$$

As proven in [6] the expectation value in eq. (2.12) is now mathematically well defined. However, if we remember the somewhat counter intuitive example of the Riemann ζ -function for $z = -1$, eq. (2.2), the physical meaning of the so evaluated expectation value $\langle \Omega \rangle$ in eq. (2.12) is completely unclear at this point.

2.1 Main result

The main – and somewhat surprising – result shown in [7] is that we actually obtain *the physical vacuum expectation value* in eq. (2.12). This statement can be summarized in the following equations where we denote by $|\psi^0\rangle$ the ground state and with $|\psi_n^0\rangle$ a discretized version of it, see in particular section 3:

$$\langle \psi^0 | \Omega | \psi^0 \rangle = \lim_{n \rightarrow \infty} \langle \psi_n^0, \Omega_n \psi_n^0 \rangle_{\mathcal{H}} \quad (2.13)$$

$$= \lim_{z \rightarrow 0} \lim_{n \rightarrow \infty} \frac{\langle (\mathfrak{G}(z)\Omega)_n \rangle}{\langle \mathfrak{G}(z)_n \rangle} \quad (2.14)$$

$$= \lim_{z \rightarrow 0} \lim_{T \rightarrow \infty + i0^+} \frac{\zeta(U(0, T)\mathfrak{G}\Omega)}{\zeta(U(0, T)\mathfrak{G})}(z) \quad (2.15)$$

$$= \langle \Omega \rangle_\zeta. \quad (2.16)$$

Eq. (2.13) tells us that we obtain the physical expectation value as the limit $n \rightarrow \infty$ from the expectation value taken in a Hilbert space \mathcal{H} evaluated in a suitable discretization scheme. Eq. (2.14) says that this is equivalent to the expectation value of the gauged observable taken at $z = 0$ in the $n \rightarrow \infty$ limit. Eq. (2.15) states that this is in turn equivalent to the ζ -trace of the path integral, i.e. the ratio of the gauged observable and time evolution operator. Finally, eq. (2.16) connects this to the definition of the ζ -regulated vacuum expectation value. Moreover, the main result given above is independent from the choice of the gauge assuming the assumptions in refs. [6, 7] are fulfilled.

2.2 The free Dirac operator example

In order to illustrate the steps that lead to the ζ -regulated vacuum expectation value let us take the example of the free Dirac operator in the continuum

$$H = \begin{pmatrix} mc^2 & -i\hbar\sigma_k\partial_k \\ -i\hbar\sigma_k\partial_k & mc^2 \end{pmatrix} \sim \begin{pmatrix} mc^2 & \hbar r\sigma_k\xi_k \\ \hbar r\sigma_k\xi_k & mc^2 \end{pmatrix} \quad (2.17)$$

where in the second step we have taken the Fourier transform expressed in radial (r) and spherical (ξ) coordinates. As a (very simple) gauge, we now consider the holomorphic function

$$g(z)(x, r, \xi) = r^z. \quad (2.18)$$

Other choices of gauges are certainly possible. For example, using a positive number δ , one may choose $r^{\delta z}f(z)(x, \xi)$, or $(1+r)^{\delta z}f(z)(x, \xi)$. Furthermore gauges of the form $f(z, r)f(z)(x, \xi)$ with $f = 1$ near $r = 0$, $f(z, r) \propto r^{\delta z}$ for $r \gg 1$, and holomorphic families of continuous functions f are common examples. But, it is sufficient to consider the simple case of eq. (2.18) here. Inserting eq. (2.17) into the general formula of the ζ -trace of eq. (2.11) we obtain see, [8],

$$\langle H \rangle = \lim_{z \rightarrow 0} \lim_{T \rightarrow \infty} \frac{\int d\omega \int dr (4mc^2 \cos(Tr) - 4ir \sin(Tr)) r^{z+2}}{\int d\omega \int dr 4 \cos(Tr) r^{z+2}} \quad (2.19)$$

which can be evaluated to

$$\langle H \rangle = mc^2 - \lim_{z \rightarrow 0} \lim_{T \rightarrow \infty} \frac{\int dr 4i \sin(Tr) r^{z+3}}{\int dr \cos(Tr) r^{z+2}}, \quad (2.20)$$

with the second term on the right hand side being zero in the limit $z \rightarrow 0$ and $T \rightarrow \infty$. Hence, we obtain for free Dirac fermions $\langle H \rangle = mc^2$. Maybe, this appears to be a most complicated way to obtain the ground state energy of the free Dirac operator, but this simple computation illustrates the steps involved in obtaining ζ -regulated vacuum expectation values through solving – possibly very high dimensional – spherical integrals. More examples can be found in [6, 7, 8].

3. Sketch of proof

In this section, we want to provide a sketch of the proof of the statement that we obtain physical vacuum expectation values. A more detailed and mathematically rigorous proof can be found in ref. [7] which is based on the results in [6]. We start with a separable Hilbert space \mathcal{H} and consider the time evolution operator

$$U(t, t') = \text{Texp} \left(-\frac{i}{\hbar} \int_t^{t'} H(s) ds \right) \quad (3.1)$$

where H is the Hamiltonian and Texp denotes the time ordered exponential. Our goal is to compute the vacuum expectation value of an observable Ω in the ground state ψ^0 of the Hamiltonian H :

$$\langle \psi^0 | \Omega | \psi^0 \rangle = \lim_{z \rightarrow 0} \lim_{T \rightarrow \infty + i0^+} \frac{\zeta(U(T, 0) \mathfrak{G} \Omega)(z)}{\zeta(U(T, 0) \mathfrak{G})(z)}. \quad (3.2)$$

The proof of eq. (3.2) proceeds by introducing nested, n -dimensional subspaces $P_n[\mathcal{H}]$ corresponding to orthogonal projections of \mathcal{H} (i.e. measurements). These nested sequences are to be taken from a discretization scheme which can be a finite or infinite lattice, a complete set of continuous functions or more general using a Schauder basis [9]. The orthogonal projections P_n are to be constructed such that the topology of \mathcal{H} is respected (think about topological sectors in QCD).

Next, we construct a Hilbert space \mathcal{H}_1 which is densely embedded in \mathcal{H} . The subspaces $P_n[\mathcal{H}]$ are to be contained in \mathcal{H}_1 and the gauge $\mathfrak{G}(z)$ as well as the gauged observable operator $\mathfrak{G}(z)\Omega$ are to be bounded operators from \mathcal{H}_1 to \mathcal{H} provided that $\text{Re}(z)$ is less than some positive real number.

If we consider a Hilbert space \mathcal{H} as a L_2 -space, then \mathcal{H}_1 will in general be a Sobolev space W_2^s , i.e. a space of functions that admit derivatives up to order s –where s is to be taken sufficiently large– and have an (integral) norm of order 2, i.e. in one dimension $\|f\|_{k,2} = \left(\sum_{i=0}^k \int |f^{(i)}(t)|^2 dt \right)^{\frac{1}{2}}$. Sobolev spaces are commonly used in the field of differential equations and we may think of taking the differential operator there (e.g. the Laplace operator) to play the role of the Hamiltonian in our problem.

Having constructed \mathcal{H}_1 , we need the orthogonal projections Q_n onto $P_n[\mathcal{H}]$ in \mathcal{H}_1 . This finally allows us to discretize the observable Ω of interest

$$\Omega_n := P_n \Omega Q_n \quad (3.3)$$

and correspondingly the discretized time evolution operator

$$U_n(t, t') = \text{Texp} \left(-\frac{i}{\hbar} \int_t^{t'} P_n H(s) Q_n ds \right) \quad (3.4)$$

which is then in $P_n[\mathcal{H}]$. Note that by “discretization” we mean here a very general discretization scheme which can be a finite or infinite lattice, a function basis (think of Fourier modes) or elements of a Schauder basis which can be considered “generalized” Fourier modes once the basis is orthonormalized.

The discretized ground state wave function is obtained by the minimum of the energy, i.e.

$$\psi_n^0 = \underset{\|\Psi_n\|=1}{\text{argmin}} \langle \Psi_n | H_n | \Psi_n \rangle \quad (3.5)$$

where $H_n = P_n H Q_n$ living in $P_n[\mathcal{H}]$. It is then possible to show [6, 7] that the discretized ground state ψ_n^0 converges to the true ground state ψ^0 .

$$\langle \psi_n^0, \psi^0 \rangle_{\mathcal{H}} \psi_n^0 \rightarrow \psi^0 \quad (n \rightarrow \infty). \quad (3.6)$$

In other words, eq. (3.6) states, fairly untrivially, that the discretized theory reproduces the infinite dimensional continuum theory in the limit $n \rightarrow \infty$ for a suitably chosen discretization scheme.

In order for this statement to hold, we need the underlying quantum field theory to have an energy gap, that H is self-adjoint, and that H plays the role of a generator of the exponential function in the time evolution operator. In a more general language, the one parameter (here the time t) exponential of an operator is considered as a semi-group and the time-dependent Hille-Yosida theorem (see theorem 5.3.1 in [10]) states under which condition the operator valued exponential has a well defined meaning, which is based on the spectrum of the considered operator.

In the discretized setup the expectation value of an observable Ω_n is given by

$$\langle \psi_n^0 | \Omega_n | \psi_n^0 \rangle = \lim_{T \rightarrow \infty + i0^+} \frac{\text{tr}(U_n(T, 0) \Omega_n)}{\text{tr}(U_n(T, 0))} \quad (3.7)$$

which takes over to the discretized gauged observable

$$\frac{\langle \psi_n^0 | (\mathfrak{G}(z) \Omega)_n | \psi_n^0 \rangle}{\langle \psi_n^0 | \mathfrak{G}(z)_n | \psi_n^0 \rangle} = \lim_{T \rightarrow \infty + i0^+} \frac{\text{tr}(U_n(T, 0) (\mathfrak{G}(z) \Omega)_n)}{\text{tr}(U_n(T, 0) \mathfrak{G}(z)_n)}. \quad (3.8)$$

Now, through the gauging procedure the operators $U(T, 0) \mathfrak{G}(z) \Omega$ and $U(T, 0) \mathfrak{G}(z)$ are of trace class in \mathcal{H} for $\text{Re}(z) \ll 0$. Furthermore, through the construction of \mathcal{H}_1 and H satisfying the Hille-Yosida theorem we can deduce that we can take the limits

$$\begin{aligned} \text{tr}(U_n(T, 0) (\mathfrak{G}(z) \Omega)_n) &\rightarrow \text{tr}(U(T, 0) \mathfrak{G}(z) \Omega) \\ \text{tr}(U_n(T, 0) \mathfrak{G}(z)_n) &\rightarrow \text{tr}(U(T, 0) \mathfrak{G}(z)). \end{aligned} \quad (3.9)$$

These limits allow us now for $\text{Re}(z) \ll 0$ to identify the ζ -regularized vacuum expectation values

$$\frac{\langle \psi_n^0 | (\mathfrak{G}(z) \Omega)_n | \psi_n^0 \rangle}{\langle \psi_n^0 | \mathfrak{G}(z)_n | \psi_n^0 \rangle} \rightarrow \lim_{T \rightarrow \infty + i0^+} \frac{\zeta(U(T, 0) \mathfrak{G} \Omega)(z)}{\zeta(U(T, 0) \mathfrak{G})(z)}. \quad (3.10)$$

In the steps above we needed the condition that $\text{Re}(z) \ll 0$ because (3.9) only holds for trace-class operators. As a last step in the proof we need to extend eq. (3.10) to all values of z with $\text{Re}(z) < \varepsilon$ when $\varepsilon > 0$ is chosen¹. For this to be true, we need that \mathfrak{G} and $\mathfrak{G} \Omega$ are bounded operators for $\text{Re}(z)$ bounded by the same positive real number ε again. A second requirement is that the norms $\|\mathfrak{G}(z) \Omega \Psi_n^0\|_{n \in \mathbb{N}}$ and $\|\mathfrak{G}(z) \Psi_n^0\|_{n \in \mathbb{N}}$ are bounded for $\text{Re}(z) < \varepsilon$ with the same ε as above. Under these conditions, the limit in eq. (3.10) holds for all values of z in a subset $\mathcal{D} \subseteq \{z \in \mathbb{C}; \text{Re}(z) < \varepsilon\}$ such that the set $\{z \in \mathbb{C}; \text{Re}(z) < \varepsilon \text{ and } z \notin \mathcal{D}\}$ contains only isolated points which guarantees the uniqueness of the analytical continuation. In more general terms, the convergence in eq. (3.10) follows from the so-called Vitali Porter theorem² see [11] chapter 2.4 which is a convergence theorem, well known in the mathematical literature which, applied to our problem at hand, guarantees the convergence in eq. (3.10). In particular, as we show in [7], the

¹This is strictly speaking more restrictive than necessary although it is very difficult to construct an example which would not satisfy this.

²According to ref. [11] this theorem was proven independently by Vitaly [12] (also published in [13]) and Porter [14].

here proposed ζ -regularized vacuum expectation value fulfills the conditions of the Vitali Porter theorem and hence the convergence in eq. (3.10) holds.

A subtlety in the proof is, whether $z = 0$ is indeed in the subset \mathcal{D} . However, in [7] it was proven that this is indeed the case. As stated in the main result, the fact that we have the convergence of eq. (2.13) we finally can relate the ζ -trace of the gauged, ζ -regulated path integral to the physical expectation value.

3.1 A note on the anomaly

The claim of our result in eq. (2.15) is that we can use the path integral in continuous Minkowski space time and obtain finite, well defined expectation values that correspond to the desired physical vacuum expectation values. This leads to the interesting question how the axial anomaly appears in this setup and how chiral gauge theories can be constructed within this approach. The short answer is that, if gauges are used that respect the (chiral) symmetry of the original theory, then the anomaly will appear through the fact that the measure is not invariant. In other words, the derivation of the anomaly will follow closely the construction of Fujikawa in [15]. To make this statement more solid and put it on a rigorous mathematical ground is subject to a work we plan to carry out in the future.

4. Quantum Computing ζ -regulated vacuum expectation values

The theoretical notion of a mathematically well defined vacuum expectation value in the path integral or in a suitably chosen discretization scheme leaves open the question, how the so obtained vacuum expectation values can be computed in practice. One direction would be to develop highly efficient methods for solving high dimensional integrals in spherical coordinates, along the line of refs. [16, 17, 18, 19, 20]. Another, very appealing and intriguing possibility is to employ quantum computations for this purpose.

In the last years, quantum computers have emerged as promising novel technologies that could be used to solve problems that are extremely difficult or even impossible to address classically. The usage of quantum computers has changed in the last years and superconducting qubit architectures such as the ones at Rigetti [21], IBM [22], or D-Wave [23] are now remotely accessible devices which can be programmed in Python with software libraries supplied by the companies. Example programs and instructions can be found on the corresponding web-pages. Also simulators are provided which can be used locally. This makes it easy to develop and test programs for correctness. The simulators also have the option to switch on noise which provides good estimates of the performance on the real hardware.

Such a setup allows to use quantum computers “easily” nowadays and provides the opportunity to test the potential of quantum computing for the particular problem one is interested in. For our case of ζ -regularized vacuum expectation values we will employ the method of variational quantum simulation, as explained in more detail below, for the problem of the 1-dimensional hydrogen atom. For the calculation we will actually employ eq. (2.13) of the main result stated above. This means that we will use a suitable discretization scheme to quantum compute the expectation value of the Hamiltonian of the 1-dimensional hydrogen atom in the ground state.

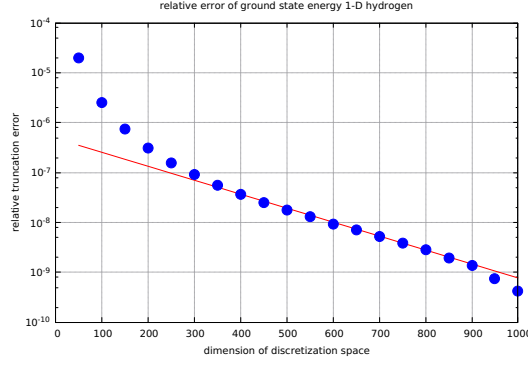


Figure 1: Results from exact diagonalization. We show the relative error Δ of the energy E when using a dimension n compared to the the largest dimension used, i.e. $n = 1024$, i.e. $\Delta = \frac{E(n) - E(1024)}{E(1024)}$.

4.1 One dimensional hydrogen atom

As anticipated above, as an example for a quantum computation we will consider here the 1-dimensional hydrogen atom with the Hamiltonian

$$H = -\frac{\partial^2}{2m} + qU(x), \quad U(x) = \begin{cases} x & ; x \in (0, \pi) \\ 0 & ; x \in (-\pi, 0] \end{cases} \quad (4.1)$$

where we restrict ourselves to the interval $(-\pi, \pi)$. The Hilbert space is $L_2(-\pi, \pi)$ and the orthogonal projection P_n maps onto the finite dimensional linear space

$$\text{lin} \left\{ \varphi_k; -\left\lfloor \frac{n}{2} \right\rfloor \leq k \leq n-1 - \left\lfloor \frac{n}{2} \right\rfloor \right\} \quad (\text{so that } \dim P_n[\mathcal{H}] = n) \quad (4.2)$$

and where $\varphi_k(x) = \frac{1}{\sqrt{2\pi}} e^{ikx}$.

The matrix elements of the 1-dimensional Hamiltonian of the hydrogen atom can be computed analytically and we obtain for $k = l$

$$\langle \varphi_k, H \varphi_k \rangle = \frac{k^2}{2m} + \frac{q\pi}{4} \quad (4.3)$$

and for $k \neq l$

$$\langle \varphi_l, H \varphi_k \rangle = \frac{q \left((-1)^{k-l} (1 - i\pi(k-l)) - 1 \right)}{2\pi(k-l)^2}. \quad (4.4)$$

Having these matrix elements at hand, we can construct the full matrix which can be exactly diagonalized, if the dimension n is not too large. In fig. 1 we show the relative error of the lowest eigenvalue, i.e. the ground state energy, with respect to the largest dimension $n = 1024$ we have used. The nice result of fig. 1 is that we see an exponentially fast convergence to the $n = \infty$ ground state energy. This is a promising result since it points to the possibility that in practice only a small number of qubits are required to obtain the ground state energy and wave function to a good accuracy.

In order to write the Hamiltonian of the hydrogen atom in a form that can be used on a quantum computer, we need to write it in terms of the Pauli matrices $\sigma^1 = \sigma_x$, $\sigma^2 = \sigma_y$, $\sigma^3 = \sigma_z$, and

$\sigma^0 = \mathbb{1}_{2 \otimes 2}$ such that the set $[\sigma^0, \sigma^1, \sigma^2, \sigma^3]$ span a *Pauli basis*

$$\{S^q = \sigma^{q_Q-1} \otimes \sigma^{q_Q-2} \otimes \dots \otimes \sigma^{q_0}; q \in 4^Q\} \quad (4.5)$$

with the exponent of four appearing because we have, in general, the possibility of all four matrices from the set $[\sigma^0, \sigma^1, \sigma^2, \sigma^3]$.

Having the matrix elements of eq. (4.4) at our disposal we can now project them onto the Pauli basis, and obtain the qubit Hamiltonian H_Q . Note that H_Q corresponds to H_n with $n = 2^Q$ in eq. (3.3)

$$H_Q = \sum_{q \in 4^Q} \frac{\text{tr}(H_{2^Q} S^q)}{2^Q} S^q. \quad (4.6)$$

H_Q is now suited to be implemented on a quantum computer. The steps described above and the qubit Hamiltonian in eq. (4.6) are very general and can be used when the matrix elements $\langle \varphi_l, H \varphi_k \rangle$ can be evaluated for a given Hamiltonian H . However, it needs to be stressed that in simpler cases, e.g. when employing the Ising or the Heisenberg model, the qubit Hamiltonian can be constructed in a much more direct and simpler way.

4.2 Variational quantum simulation

One frequently used way to obtain the ground state energy and wave function on a quantum computer is the method of variational quantum simulations see, e.g. [24]. In this approach, an initial state vector $|\Psi_{\text{init}}\rangle$ is generated first. On this state vector a sequence of gate operations is applied which are single qubit unitary operations $e^{-iS\theta}$ depending on a parameter θ and with S being the Pauli matrices or, e.g., a Hadamard gate. Moreover, we can have entanglement gates such as a (parametric) CNOT gate.

In this way, a state vector $|\Psi(\vec{\theta})\rangle$ depending on all parameters of the applied unitary gate operations is generated,

$$|\Psi(\vec{\theta})\rangle = e^{-iS_{(n)}\theta_n} \dots e^{-iS_{(1)}\theta_1} |\Psi_{\text{init}}\rangle. \quad (4.7)$$

Defining $R_j := e^{-iS_{(j)}\theta_j}$ a (energy) cost function C can be computed

$$C := \left\langle \Psi_{\text{init}} \left| \left(\prod_{j=1}^n R_j \right)^\dagger H \prod_{j=1}^n R_j \right| \Psi_{\text{init}} \right\rangle. \quad (4.8)$$

The goal is then to minimize this cost function over the vector of parameters $\vec{\theta}$. The employed strategy is to evaluate the cost function on the quantum computing hardware while the minimization over the variational parameters is performed on a classical computer.

In our original work [7], we tried to use the libraries that were provided in the python software package of Rigetti to minimize the cost function built from the 1-dimensional hydrogen Hamiltonian, see refs. [25, 26] for a discussion of variational eigensolvers within the Rigetti framework. However, in today's NISQ (Noisy Intermediate Scale Quantum computers) area, we were not successful to obtain any meaningful result on the real hardware.

We therefore resorted to a more straightforward method consisting of a sequential update of single parameters θ_k . In particular, we divided each $\theta_k \in [0, 2\pi]$ into N steps

$$\theta_k = 2\pi i/N \pm \varepsilon, \quad k = 1, \dots, N \quad (4.9)$$

with $\varepsilon < \pi/N$ some random noise. We then visited each θ_k separately, minimized the energy for this θ_k and proceeded to the next angle. Sweeping in this way several times over all angles θ_k allowed us to eventually obtain the targeted minimum of the cost function in eq. (4.8).

For the quantum hardware computations we used Rigetti's 8 qubit Agave chip. In particular, we selected the qubit with the best measured fidelity and implemented the qubit Hamiltonian of eq. (4.6). While this approach worked for 1 qubit successfully and we could obtain an about 95% accuracy for the ground state energy, we were not able to achieve a significant result for 2 qubits.

In order to improve this –rather disappointing– result we implemented a gradient descent algorithm to find the minimum of the cost function in eq. (4.8). The gradient of the cost function can be obtained through the differentiation with respect to the parameters θ_k and the gradient vector can then actually be computed on the quantum hardware itself.

Let us for illustration purposes consider the cost function for 2 unitaries only

$$C := \left\langle \psi_{\text{init}} \left| \left(e^{i\sigma^1 \theta_1} e^{i\sigma^2 \theta_2} \right)^\dagger H e^{i\sigma^1 \theta_1} e^{i\sigma^2 \theta_2} \right| \psi_{\text{init}} \right\rangle. \quad (4.10)$$

Then the gradient vector is obtained as

$$D = \left(\frac{\partial C}{\partial \theta_1}, \frac{\partial C}{\partial \theta_2} \right). \quad (4.11)$$

E.g., the derivative with respect to θ_1 is given by

$$\frac{\partial}{\partial \theta_1} C = \left\langle \psi_{\text{init}} \left| \left(e^{i\sigma^1 \theta_1} e^{i\sigma^2 \theta_2} \right)^\dagger \left[(i\sigma^1)^\dagger H + H(i\sigma^1) \right] e^{i\sigma^1 \theta_1} e^{i\sigma^2 \theta_2} \right| \psi_{\text{init}} \right\rangle, \quad (4.12)$$

where we commuted the Pauli matrix σ^1 through the unitaries, when necessary. This means that we can re-use the already generated state vector and measure $(i\sigma^1)^\dagger H + H(i\sigma^1)$ directly on the quantum hardware. A gradient descent algorithm can then be constructed to obtain a new state vector $\vec{\theta}^{\text{new}}$ through

$$\vec{\theta}^{\text{new}} := \vec{\theta}^{\text{old}} - \eta \nabla C(\vec{\theta}^{\text{old}}) \quad (4.13)$$

with a tunable learning rate η . Note that the steps above can be generalized to much more complicated circuits. For example, when a CNOT gate is used, it can be expressed in terms of Pauli matrices again. Hence, the Pauli matrix originating from a differentiation can again be commuted through the CNOT entanglement gate and we find a similar structure as in eq. (4.12), although with a more complicated operator to be measured for the evaluation of the gradient.

With the approach of this *global* gradient descent algorithm and Rigetti's new hardware [21] we could get results also for 2 qubits with a 90% fidelity for the ground state wave function. However, the 3-qubit case was unfortunately not successful. In addition, the global algorithm sketched above is suitable for a small number of qubits only. For many qubits, the measurements

become very difficult since the scaling of the algorithm is exponential. Hence, alternative new methods and algorithms need to be developed and work in this direction is in progress.

5. Conclusion

In this proceeding we have shown that the ζ -regularization leads to a mathematically well defined, non-perturbative expression of Feynman's path integral in a Minkowski (or more general) metric. Within this ζ -regularization vacuum expectation values can be computed and we sketched a proof that these are the physical vacuum expectation values.

From a practical side, a vacuum expectation value can be computed in two ways based on our main result, eqs. (2.13)-(2.16). When using eq. (2.15) in the Fourier integral kernel representation a high dimensional spherical integral needs to be solved. When employing eq. (2.13) the vacuum expectation value is obtained through a limit procedure of an appropriate discretization scheme. Here, the ground state energy and wave function can be computed –at least in principle– either by tensor network methods or by employing a quantum computer, see ref. [27] and ref. [28] for applications in high energy physics, respectively.

In the present work we evaluated the ground state energy of a 1-dimensional hydrogen atom on a quantum computer through the hybrid classical-quantum approach of a variational quantum eigensolver. Although we could demonstrate that this method works in practice to compute the energy as a vacuum expectation value, the number of qubits that we could use has been very small.

The here presented framework of the ζ -regularization of the path integral is still novel and only very first steps have been taken to explore this approach to quantum field theories. In order to develop both, the conceptual as well as the practical aspects of the ζ -regularization further, a number of main steps (our “wishlist”) need to be developed in the future:

- It would be very desirable to explore more problems where the ζ -regularization can be exploited from a theoretical point of view. Examples are the application in perturbation theory, curved space-time, or looking at chiral gauge theories.
- From a practical side, in order to evaluate the ζ -regulated path integral, efficient methods are needed to solve high-dimensional spherical integrals to obtain expectation values of physical observables in a quantitative way.
- Working in a Hamiltonian approach using a suitable discretization scheme, novel algorithms for tensor networks and quantum computations need to be developed. In particular, in the latter case algorithms are needed which are efficient, scalable, and robust against errors of the used quantum device.
- Finally, better quantum hardware need to be built with a high qubit fidelity and optimally even with error correction.

Acknowledgment

We thank P. Stornati for very useful discussions on the gradient descent part of this work.

References

- [1] R. P. Feynman. Space-Time Approach to Non-Relativistic Quantum Mechanics. *Rev. Mod. Phys.*, 20:367–387, 1948.
- [2] R. P. Feynman, A. R. Hibbs, and D. F. Styer. *Quantum Mechanics and Path Integrals*. Dover Publications, Inc., 2005.
- [3] G. Margazoglou, L. Biferale, R. Grauer, K. Jansen, D. Mesterházy, T. Rosenow, and R. Tripiccione. A Hybrid Monte Carlo algorithm for sampling rare events in space-time histories of stochastic fields. *Phys. Rev.*, E99(5):053303, 2019.
- [4] H. J. Rothe. Lattice gauge theories: An Introduction. *World Sci. Lect. Notes Phys.*, 43:1–381, 1992. [World Sci. Lect. Notes Phys.82,1(2012)].
- [5] Christof Gattringer and Christian B. Lang. Quantum chromodynamics on the lattice. *Lect. Notes Phys.*, 788:1–343, 2010.
- [6] T. Hartung. Regularizing Feynman Path Integrals using the generalized Kontsevich-Vishik trace. *J. Math. Phys.*, 58:123505, 2017.
- [7] Tobias Hartung and Karl Jansen. Zeta-regularized vacuum expectation values. *J. Math. Phys.*, 60(9):093504, 2019.
- [8] T. Hartung and K. Jansen. Integrating Gauge Fields in the ζ -formulation of Feynman’s path integral. *to appear in a volume in the series Applied Numerical and Harmonic Analysis in honor of Luigi Rodino*, 2019. arXiv:1902.09926.
- [9] B. Beauzamy. *Introduction to Banach Spaces and their Geometry*. Elsevier Science Publishers, 1985.
- [10] A. Pazy. *Semigroups of Linear Operators and Applications to Partial Differential Equations*. Springer, 1992.
- [11] J.L. Schiff. *Normal Families*. Springer, New York, 1993.
- [12] G. Vitali. Sopra le serie di funzioni analitiche. *Rend. della R. Inst. Lombardo di Sci. Lett.*, 2(36):772, 1903.
- [13] G. Vitali. Sopra le serie di funzioni analitiche. *Ann. Mat. Pura Appl.*, 3(10):65, 1904.
- [14] M.B. Porter. Concerning series of analytic functions. *Ann. Math.*, 2(6):190, 1904.
- [15] Kazuo Fujikawa, Shuichi Ojima, and Satoshi Yajima. On the Simple Evaluation of Chiral Anomalies in the Path Integral Approach. *Phys. Rev.*, D34:3223, 1986.
- [16] Harald Niederreiter. *Random number generation and quasi-Monte Carlo methods*, volume 63 of *CBMS-NSF Regional Conference Series in Applied Mathematics*. Society for Industrial and Applied Mathematics (SIAM), Philadelphia, PA, 1992.
- [17] F. Kuo, Ch. Schwab, and I. Sloan. Quasi-monte carlo methods for high-dimensional integration: the standard (weighted hilbert space) setting and beyond. *ANZIAM Journal*, 53(0), 2012.
- [18] K. Jansen, H. Leovey, Andreas Ammon, A. Griewank, and M. Muller-Preussker. Quasi-Monte Carlo methods for lattice systems: a first look. *Comput. Phys. Commun.*, 185:948–959, 2014.
- [19] A. Ammon, A. Genz, T. Hartung, K. Jansen, H. Leovey, and J. Volmer. On the efficient numerical solution of lattice systems with low-order couplings. *Comput. Phys. Commun.*, 198:71–81, 2016.

- [20] A. Ammon, T. Hartung, K. Jansen, H. LeÁúvey, and J. Volmer. Overcoming the sign problem in one-dimensional QCD by new integration rules with polynomial exactness. *Phys. Rev.*, D94(11):114508, 2016.
- [21] Rigetti Computing. <https://www.rigetti.com>.
- [22] IBM Quantum Computing. <https://www.ibm.com/quantum-computing/>.
- [23] D-WAVE Computing. <https://www.dwavesys.com>.
- [24] A. Peruzzo et al. A variational eigenvalue solver on a photonic quantum processor. *Nature Communications*, 5, 2016.
- [25] N. C. Rubin. A hybrid classical/quantum approach for large-scale studies of quantum systems with density matrix embedding theory. arXiv:1610.06910v2 [quant-ph], 2016.
- [26] M. Reagor, C. B. Osborn, N. Tezak, A. Staley, G. Prawiroatmodjo, M. Scheer, N. Alidoust, E. A. Sete, N. Didier, M. P. Da Silva, E. Acala, J. Anegeles, A. Bestwick, M. Block, B. Bloom, A. Bradley, C. Bui, S. Caldwell, L. Capelluto, R. Chilcott, J. Cordova, G. Crossman, M. Curtis, S. Deshpande, T. El Bouayadi, D. Girshovich, S. Hong, A. Hudson, P. Karalekas, K. Kuang, M. Lenihan, R. Manenti, T. Manning, J. Marshall, Y. Mohan, W. O’Brien, J. Otterbach, A. Papageorge, J. P. Paquette, M. Pelstring, A. Polloreno, V. Rawat, C. A. Ryan, R. Renzas, N. Rubin, D. Russel, M. Rust, D. Scarabelli, M. Selvanayagam, R. Sinclair, R. Smith, M. Suska, T. W. To, M. Vahidpour, N. Vodrahalli, T. Whyland, K. Yadav, W. Zeng, and C. T. Rigetti. Demonstration of universal parametric entangling gates on a multi-qubit lattice. *Sci. Adv.*, 4:eao3603.
- [27] Mari Carmen Banuls and Krzysztof Cichy. Review on Novel Methods for Lattice Gauge Theories. 2019.
- [28] M. C. Banuls et al. Simulating Lattice Gauge Theories within Quantum Technologies. 2019.